Eur. J. Mineral.
2002, **14**, 915-928

Garnet-biotite-clinozoisite gneiss: a new type of diamondiferous metamorphic rock from the Kokchetav Massif

ANDREI V. KORSAKOV[1*], VLADISLAV S. SHATSKY[1], NIKOLAY V. SOBOLEV[1] and ANTON A. ZAYACHOKOVSKY[2]

[1.]United Institute of Geology, Geophysics and Mineralogy, Novosibirsk 630090, Russia
[2.]Nedra Geologic Expedition 475013 Kokchetav, Kazakhstan

Abstract: Clinozoisite gneisses were studied from the Barchi-Kol area, located 17 km to the west of the Kumdy-Kol microdiamond deposit at Kokchetav massif (Northern Kazakhstan). As distinct from the deposit, the studied rocks are characterized by predominance of diamonds of octahedral habit. Ultrahigh-pressure mineral assemblages were investigated mainly as inclusions in zircons from these rocks. It is established that nucleation and growth of some zircon grains began at the peak of metamorphism (T = 950-1000°C and P > 40 kbar) and continued while temperature and pressure decreased to T = 650-750°C and P = 10-12 kbar. Ultrahigh-pressure metamorphic conditions for clinozoisite gneisses from the Barchi-Kol area are comparable with those for the Kumdy-Kol microdiamond deposit and correspond to T = 900-1000°C and P > 40 kbar. High P-T of metamorphism and bulk-rock composition did not affect the morphology of the diamond crystals. The abundance of fluid or melt is proposed to be responsible for the variable extent of the completeness of cuboid reshape reaction, resulting in the formation of octahedral diamond crystals. The preservation of coesite as inclusions within zircon grains, as well as within garnets, suggests the rapid cooling and fast exhumation of the studied rocks. Based on concentration profiles in garnets from diamondiferous clinozoisite rocks, the duration of retrograde metamorphism is estimated to be less than 0.1 Ma.

Key-words: diamond, coesite, UHPM, zoisite-quartz symplectite, zircon.

Introduction

The Kokchetav Massif is a unique object for study of crustal rocks which have experienced ultrahigh-pressure metamorphism (P > 28 kbar, *e.g.* Chopin & Sobolev, 1995). The reasoning is as follows. Firstly, diamond and coesite are widespread in the form of inclusions in the rock-forming and accessory minerals of various rock types of the Zerenda series (Dobretsov *et al.*, 1995; Shatsky *et al.*, 1995). Secondly, the area of occurrence of diamondiferous rocks exceeds 200 km^2 (Shatsky *et al.*, 1991). Diamondiferous rocks and diamonds of the Kumdy-Kol microdiamond deposit have been investigated previously in detail (Sobolev & Shatsky, 1987, 1990; Shatsky & Sobolev, 1993; Ekimova *et al.*, 1994; Shatsky *et al.*, 1995; Zhang *et al.*, 1997; Shatsky *et al.*, 1998a, 1999; De Corte *et al.*, 1998; Katayama *et al.*, 2000). In particular, it has been shown that, as a rule, the minerals corresponding to ultrahigh-pressure (highest-grade) metamorphism remain only as inclusions in zircons and garnets (Sobolev *et al.*, 1991, 1994; Korsakov *et al.*, 1998; Shatsky *et al.*, 1998b). There exists also independent evidence that the diamondiferous rocks were metamorphosed under pressures corresponding to the diamond stability field. At the same time, some questions concerning the evolution of UHP metamorphic complexes remain to be answered. (1) Are there variations in P-T of metamorphism of the diamondiferous rocks in the western block? (2) Which stage gives rise to zircons used for dating high-pressure metamorphism? (3) What factors are responsible for the morphological diversity of diamonds in rocks of different petrographic type? (4) What is the rate of exhumation of high-pressure rocks? To answer these questions, we studied clinozoisite rocks of the Barchi-Kol diamondiferous area. The geological setting of this area has much in common with the Kumdy-Kol deposit. At the same time, the predominance of diamonds of octahedral habit is a characteristic feature of the Barchi-Kol clinozoisite rocks, as distinct from the Kumdy-Kol rocks.

Mineral abbreviations used in this paper are after Kretz (1983), with the exception of the following: Dia-diamond, Coe-coesite, Czo-clinozoisite, Phe-phengite, Zrn-zircon.

Geological setting

The Kokchetav Massif is considered to be a zone of tectonic megamelange, composed of seven blocks (Tectonic Units 1 to 7) with varying lithologies and

*corresponding author, e-mail: korsakov@uiggm.nsc.ru

0935-1221/02/0014-0915 $ 6.30
DOI: 10.1127/0935-1221/2002/0014-0915

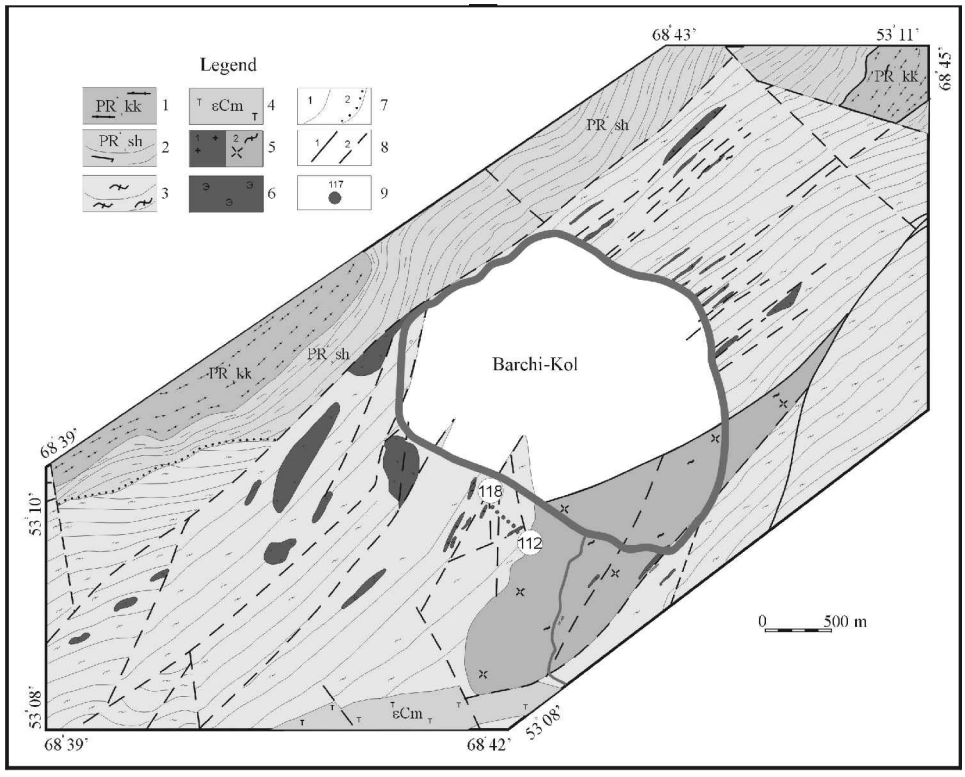

Fig. 1. A geological sketch map of the Barchi-Kol site compiled by A.A. Zayachkovsky on the basis of the drilling data obtained by the Kokchetav Prospecting Expedition. Symbols: 1 - Quartzites, sericite-quartz schists (Kokchetav Formation); 2 - Sericite-chloritic, carbon-micaceous, carbon-carbonate schists, limestones (Sharyk Formation); 3 - Kyanite, clinopyroxene, clinozoisite, biotite-bearing and two-mica gneisses; garnet-pyroxene and silicate-carbonate rocks; amphibolites, migmatites (Tectonic Unit 1); 4 - Pyroxenites, micaceous pyroxenites, carbonatites (Barchi Massif, Krasnomai alkali-utrabasic complex); 5 - (1) Leucocratic fine-grained granites, alaskitic granites. Granitoid dykes and veins of the Borovsky complex (S-D); (2) granite-gneisses; 6 - Eclogites; 7 - Geological boundaries: (1) concordant sequences of rocks; (2) drastically discordant sequences; 8 - Tectonic disturbances: (1) Regional, established from survey at a scale of 1:50,000; (2) Inferred from geophysical data and confirmed by observations; 9 - Numbered boreholes.

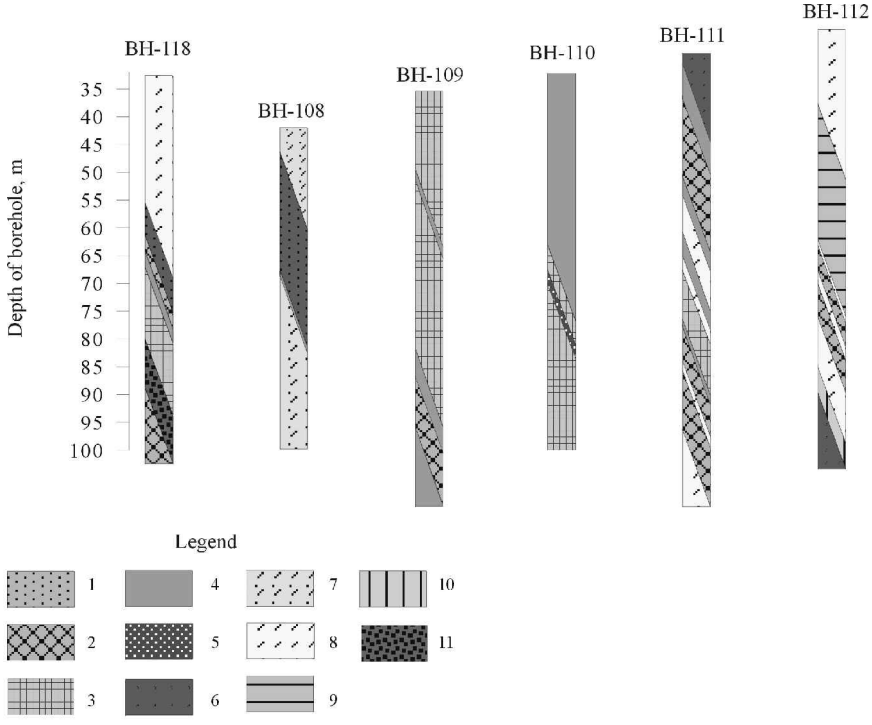

Fig. 2. A geological section of part of the Barchi-Kol terrain, constructed on the basis of the drilling data obtained by the Kokchetav Prospecting Expedition. (The boreholes are 50 m apart from one another). The symbols are: (1) - Garnet-biotite gneisses with plagioclase (**Grt-Bt-Kfs-Qtz**-*Pl*+Cal+*Chl*); (2) - Garnet-biotite gneisses (**Grt-Bt-Kfs-Qtz**+Cal+*Chl*); (3) - Pyroxene gneisses (**Grt-Cpx-Bt-Kfs-Qtz** +Cal+*Amp*+*Pl*+*Chl*); (4) - Clinozoisite gneisses (**Grt-Czo-Bt-Kfs-Qtz**+Cpx+Cal +*Amp*+*Pl*+*Chl*); (5) - Kyanite gneisses (**Grt-Ky-Bt-Kfs-Qtz**+Cpx+Cal+*Chl*); (6) - Eclogites (**Grt-Cpx-Qtz**+Cal+*Amp* +*Bt*+*Pl*+*Chl*); (7) - Garnet-biotite quartz rocks (**Grt-Bt-Qtz**+Cal+*Chl*); (8) - Biotite-K-feldspar-quartz (Bt-Kfs-Qtz); (9) - Quartz-mica schists (Qtz-Ms); (10) - Quartz-K-feldspar rocks (Qtz-Kfs); (11) - quartz-tourmaline rocks (Qtz-Tur).

Table 1. Chemical compositions of clinozoisite gneisses, determined by XRF (analyst L.D. Kholova).

Sample	SiO_2	TiO_2	Al_2O_3	$Fe_2O_3^{\#}$	MnO	MgO	CaO	Na_2O	K_2O	P_2O_5	LOI	Total
B93-6*	55.94	0.53	11.38	3.87	0.16	5.8	10.43	0.11	4.71	0.19	6.44	99.56
B94-118	57.41	0.55	12.51	7.47	0.17	8.67	5.33	0.25	3.03	0.04	4.6	100.03
B94-369*	64.56	0.46	10.72	2.95	0.16	6.88	6.7	0.13	3.27	0.06	4.16	100.05
B94-156*	65.37	0.42	11.25	3.43	0.16	6.52	7.41	0.08	2.75	0.17	2.43	99.99
B94-83*	65.54	0.42	10.84	4.34	0.16	6.96	4.76	0.44	3.09	0.14	3.27	99.96
B95-38	66.85	0.64	13.45	4.1	0.12	4.02	0.75	0.63	6.78	0.05	2.35	99.74
B94-331a*	67.19	0.47	11.3	3.37	0.15	5.64	5.16	0.25	3.52	0.05	2.81	99.91
B95-41	67.3	0.67	13.84	3.69	0.12	3.21	0.62	0.5	6.78	0.14	2.97	99.84
B95-3	69.48	0.48	10.75	3.06	0.12	4.04	3.18	0.77	4.38	0.07	3.56	99.89
B95-33	70.2	0.5	11.32	3.69	0.13	5.22	1.89	0.11	4.64	0.03	2.14	99.87
114-100	70.46	0.48	10.95	3.51	0.13	5.62	2.81	0.61	3.91	0.03	2.01	100.52
B95-26	70.57	0.57	11.64	3.48	0.12	4.89	1.79	0.4	4.73	0.02	1.83	100.04
B95-28	70.63	0.39	9.31	4.71	0.14	6.03	3.66	0.47	2.47	0.06	2.08	99.95
B95-17	71.05	0.48	10.64	3.41	0.12	4.82	2.08	0.5	4.49	0.04	2.23	99.86
B94-347	71.57	0.41	9.26	4.8	0.14	5.23	3.36	0.23	2.17	0.04	2.69	99.9
B95-30	71.91	0.49	10.87	3.65	0.13	4.91	1.93	0.36	4.03	0.04	1.62	99.94
B95-19	73.19	0.44	10.44	3.49	0.13	4.6	1.56	0.52	4.09	0.05	1.47	99.98
B95-29	73.54	0.42	9.58	4.16	0.14	5.14	2.26	0.23	3.25	0.04	1.21	99.97
B94-331	73.57	0.38	9.1	4.29	0.13	5.15	2.76	0.09	2.76	0.03	1.71	99.97

*- samples, where rock-forming minerals were analyzed, as well as mineral inclusions in zircons and garnets. $^{\#}$- All Fe as Fe_2O_3.

different conditions of metamorphism (Dobretsov *et al.*, 1995, 1998; Theunissen *et al.*, 2000). Diamondiferous rocks are recorded reliably only within Unit 1, which is composed of garnet-bearing gneisses and schists with interlayers of carbonate rocks and isolated bodies of eclogite and amphibolite (Dobretsov *et al.*, 1995; Shatsky *et al.*, 1995; Claoue-Long *et al.*, 1991). The Barchi-Kol area lies 17 km west of the Kumdy-Kol microdiamond deposit. According to drilling data by the Kokchetav Geological Prospecting Expedition (Lavrova *et al.*, 1996; Massago, 2000), the Barchi-Kol area is a fragment of a metasedimentary terrain , dipping 70° to the southeast (Fig. 1 and 2). The following rocks are recorded in this area: eclogites, garnet-pyroxene rocks, amphibolites, calc-silicate rocks, migmatites, schists and gneisses. In turn, the gneisses are subdivided into kyanite, clinopyroxene, clinozoisite, biotite, and two-mica bearing varieties. The calc-silicate rocks are interlayered with garnet-biotite gneisses. The eclogites and amphibolites occur as boudins up to 10 m in thick in the matrix of gneisses and schists.

The diamondiferous clinozoisite gneisses occur as lenses or thin beds (0.5 to 10 m) among biotite gneisses and schists, as well as within calc-silicate rocks. The relationships between different petrographic types are shown in more detail in the borehole sections of Fig. 2. The majority of the rocks are almost completely altered under greenschist-facies conditions; the relics of primary high-pressure assemblages are preserved only as inclusions in garnet and zircon.

Whole-rock XRF-derived compositions of clinozoisite gneisses are given in Table 1. The protolith of these gneisses could be Ca-rich clays. Similar rocks have been documented in North America, near Lake Superior (Cullers, 1994).

Samples and methods

Petrography and diamond distribution were examined in thin sections and plane-parallel plates polished on both sides. More than 1500 plates and thin sections were observed and described. Inclusions in zircons and garnets were examined in thin-section-like plates. For this purpose, rock fragments weighing 4 to 50 g were crushed to a fraction less than 0.25 mm. After treatment by heavy liquids, a concentrate remained from which zircons and garnets were removed and then mounted onto thin sections. The technique of making these preparations is described in more detail in Sobolev *et al.* (1991). The minerals were analysed using a Camebax microprobe. To identify coesite and diamond unambiguously, the minerals were additionally examined by Raman spectroscopy using a multichannel spectrometer (Jobin-Yvon Omars-89, France). Zonation in zircons was investigated by cathode luminescence (CL) with a scanning electron microscope (Jeol JSM 35).

Petrography

The examined gneisses were drastically altered during the retrograde stage of metamorphism. At that stage, these rocks contained abundant inclusions of coesite in garnets. The main rock-forming minerals of the clinozoisite

Table 2. Mineral assemblages of clinozoisite gneisses and mineral inclusions in zircons and garnets.

Sample	Grt	Cpx	Amp	Czo	Bt	Phe	Kfs	Pl	Ky	Dia	Coe	Qtz	Chlt	Cal
B93-6	*+	*+		*	*	+	*+	×	*+	+×	+	*+×	*+×	*+×
B94-83	*+			*	*+		*			+×	+×	*+×	*	*×
B94-118	*+			*sym	*					+×		*×	*×	*×
B94-156	*+	*+×	+	*	*		*+			+×	+×	*+	*+	*+
B94-331	*+	*+		*	*+		*+			+×		*+	*+	*+
B94-331a	*+			*	*+		*			+×	+×	*+	*+	*+
B94-347	*+	*+		*	*+		*			+×	+	*+	*+×	*+
B94-369	*+	*+		*	*+×		*+			+×	+×	*+	*+	*+
B95-42	*+	*+×	+	*sym	*+×	+×	*+	.		+×	+	*+	*+	*+

* - Rock-forming minerals
\+ and × - Mineral inclusions in zircon and garnet respectively
sym-Quartz-clinozoisite symplectite

gneisses are quartz (10-60 %), biotite (10-40 %), garnet (5-30 %), clinozoisite (5-20 %), clinopyroxene (0-15 %) and K-feldspar (5-10 %). Also present are kyanite, amphibole, chlorite, calcite, and/or tourmaline; the accessory minerals are zircon, rutile, sphene, apatite, and/or graphite. The mineral assemblages occurring as inclusions in zircon and garnet, as well as in the matrix, are presented in Table 2. The rocks have a lepidogranoblastic texture and a massive structure. In some gneiss samples, there are alternating bands of dark (biotite) and light (clinozoisite, clinopyroxene)material, with thicknesses of 1-3 mm to 1-2 cm. In one of the samples, these bands are microfolded.

Garnet is represented by light-pink subeuhedral or flattened grains 50 μm to 3 mm in size. Only the minute crystals found in quartz-enriched interlayers are euhedral. In addition, atoll garnets were found. The inner part of such crystals is composed of quartz, calcite and biotite with, less frequently, an aggregate of these minerals. An initial stage of the formation of atoll garnets is shown in Fig. 3. In this case, all the individual grains are idiomorphic, and the matrix is represented by quartz. At subsequent stages, the garnets composing the atolls develop in size to become large porphyroblasts. Most of the garnet grains contain abundant mineral inclusions: biotite, phengite, coesite, clinopyroxene, diamond, graphite, calcite, chlorite and quartz. The inclusions are irregularly distributed within the garnet grains. Mica-carbonate, chlorite-carbonate or biotite occur as pseudomorphs after garnet, with rather common relics of the latter.

Clinozoisite forms elongated colourless crystals which show an oblique extinction in thin sections, with an angle Ng^**C** less than 12°. In some samples, clinozoisite is represented by single crystals, while in other samples it intergrows with quartz to form a quartz-clinozoisite symplectite (Fig. 4). The quartz segregations may vary drastically in size, but the quantitative relation between quartz and clino-

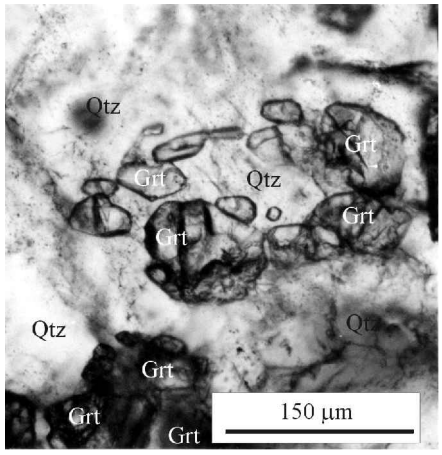

Fig. 3. Initial stage of formation of atoll-like garnet.

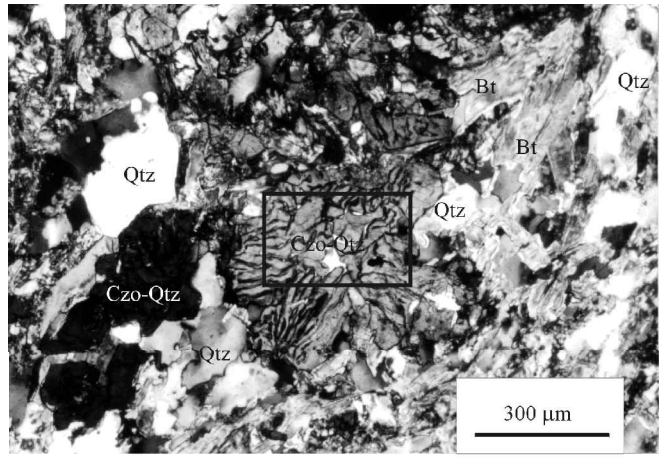

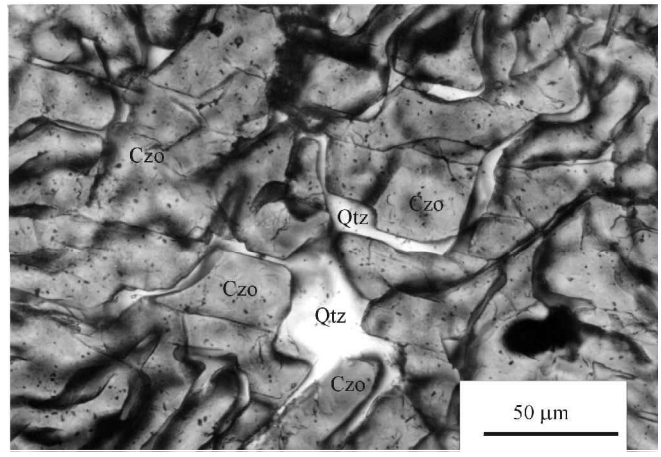

Fig. 4. Quartz-clinozoisite symplectite (crossed nicols). (b) detail of (a).

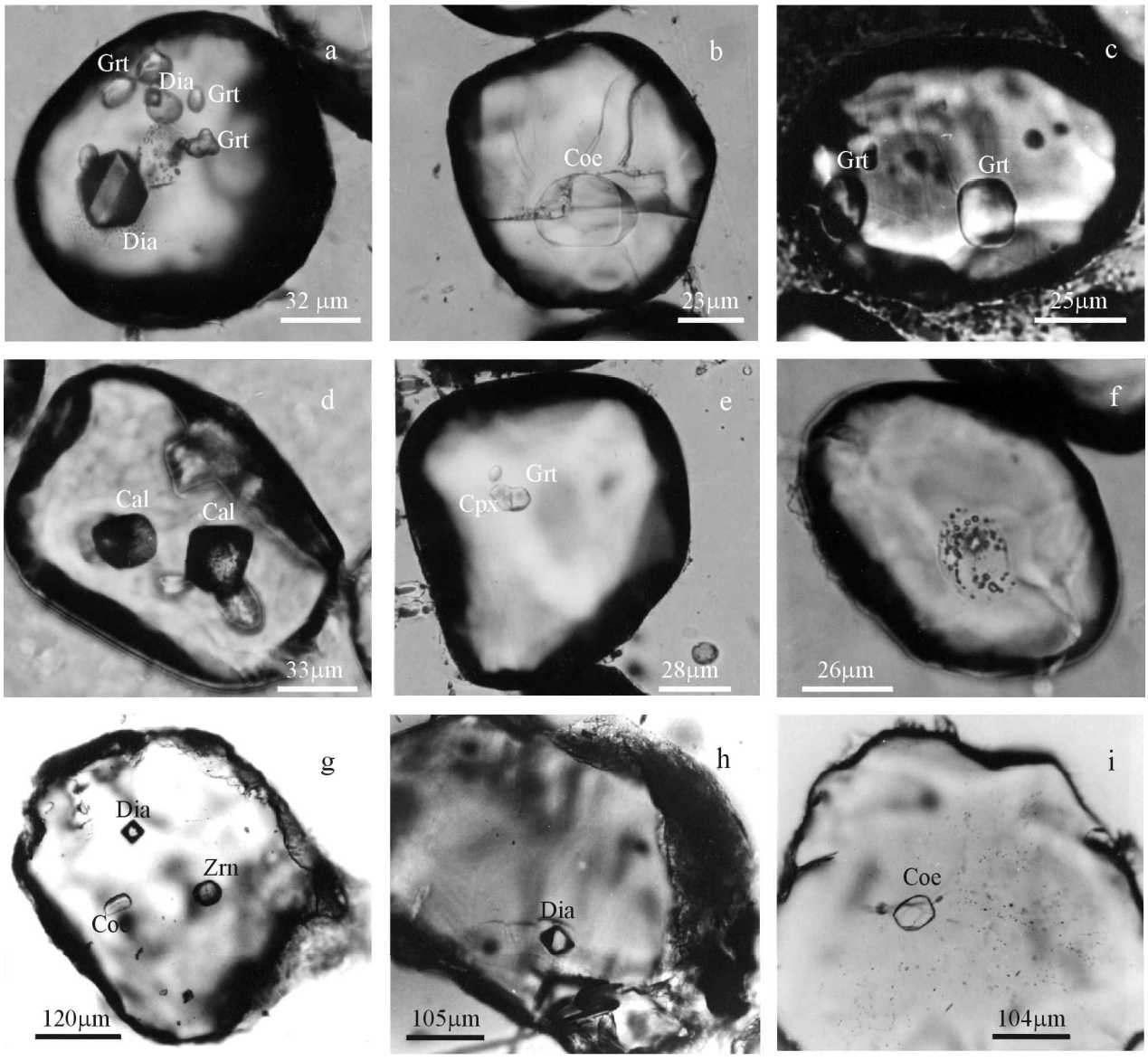

Fig. 5. Mineral inclusions in grains of zircon and garnet. (a) Inclusions of diamond and garnet in zircon. The core of the grain contains a cluster of minute solid-phase inclusions, which give way to large inclusions of garnet and diamond at the rim (B93-6); (b) Inclusion of coesite in zircon (B94-83); (c) Zoned zircon with garnet inclusions from the clinozoisite gneiss sample B94-331a. The compositions of garnets are given in Table 3 - 49-17 and 49-18, here shown on left and right, respectively; (d) Inclusions of magnesian calcites in zircon (B93-6); (e) Clinopyroxene-garnet intergrowth in zircon (B94-369); (f) Cluster of non-identified mineral inclusions in the core of a zircon grain (B93-6); (g) Inclusions of diamond, coesite and zircon in garnet (B94-83); (h) Octahedral diamond crystal in garnet (B94-83); (i) Coesite inclusion in garnet (B94-83).

zoisite remains nearly constant (1:3). Although the rock may contain up to 20 % clinozoisite, this mineral was only found once as an inclusion in garnet, intergrown with calcite and biotite.

Biotite determines the rock appearance and is found as light-brown flakes up to 2 mm in sizewith chlorite and a mica-carbonate aggregate replacing it. A fine-grained aggregate of biotite, chlorite and calcite forms pseudomorphs after garnet. White micas have not been identified among the rock-forming minerals of the gneisses.

Clinopyroxene occurs as colourless subhedral grains, which have a slight greenish tint when they are replaced by a mica-carbonate-chlorite aggregate. Biotite, calcite and quartz are identified as inclusions in clinopyroxenes, but diamond inclusions are not found.

Colourless kyanite crystals with diamond inclusions are observed in only one sample. A mica-chlorite aggregate develops along the boundaries of all kyanite grains. Therefore, there are no direct contacts between kyanite and other minerals such as clinopyroxene, clinozoisite or K-feldspar, although grains of all these minerals occur at a distance of less than 0.5 mm from one another.

K-feldspar is usually weakly sericitized, but in some samples it is completely altered. Along with quartz, it

Table 3. Compositions of mineral intergrowths, occurring as inclusions in zircons.

Sample	B94-83	B94-369				B93-6				B95-42	
№	26-60	21-81	21-80	7-57	7-58	18-130	18-131	87-150	8-162	30-15	30-16
Site	r	m	c	m	m	m	m	m	c	m	m
Mineral	Grt*	Grt	Bt	Grt	Cpx	Cal	Amp	Cpx*	Grt*	Cpx	Amp
SiO_2	39.0	40.0	37.8	41.4	53.2	0.13	50.6	55.3	40.6	54.4	45.6
TiO_2	0.03	0.05	1.93	0.00	0.02	0.01	0.49	0.22	0.04	0.14	0.27
Al_2O_3	21.5	21.3	15.2	22.5	5.57	0.00	7.4	16.4	22.1	9.7	16.1
FeO	16.8	15.6	9.24	10.97	1.83	0.96	6.97	2.45	14.5	2.53	6.59
MnO	1.99	3.13	0.25	0.66	0.05	0.67	0.22	0.26	1.21	0.06	0.08
MgO	8.45	7.27	18.81	11.32	14.41	1.59	18.19	7.36	9.76	11.9	14.2
CaO	11.1	11.9	0.02	13.5	23.1	56.5	12.1	12.4	11.7	17.9	11.3
Na_2O	0.02	0.02	0.07	0.00	0.81	0.02	0.93	5.50	0.03	3.05	2.09
K_2O	0.00	0.11	9.51	0.00	0.04	0.02	0.10	0.00	0.02	0.16	1.04
Total	98.88	99.37	92.79	100.26	98.98	59.86	97.00	99.96	100.00	99.83	97.26
Si	3.00	3.05	2.88	3.04	1.94	0.00	7.20	1.96	3.03	1.94	6.55
Ti	0.00	0.00	0.11	0.00	0.00	0.00	0.05	0.01	0.00	0.00	0.03
Al	1.95	1.92	1.36	1.94	0.24	0.00	1.24	0.69	1.95	0.41	2.72
Fe	1.08	1.00	0.59	0.67	0.06	0.01	0.83	0.07	0.90	0.08	0.79
Mn	0.13	0.20	0.02	0.04	0.00	0.01	0.03	0.01	0.08	0.00	0.01
Mg	0.97	0.83	2.14	1.24	0.78	0.04	3.86	0.39	1.09	0.63	3.04
Ca	0.91	0.98	0.00	1.06	0.90	0.94	1.85	0.47	0.94	0.69	1.73
Na	0.00	0.00	0.01	0.00	0.06	0.00	0.26	0.38	0.00	0.21	0.58
K	0.00	0.01	0.92	0.00	0.00	0.00	0.02	0.00	0.00	0.01	0.19

*- intergrowth with quartz; c, m, r – core, mantle and rim respectively

forms a fine-grained matrix, in which are observed larger segregates of the above-mentioned minerals . The majority of the quartz grains show a wavy extinction and serrated boundaries.

Tourmaline is represented by rare crystals with abundant inclusions of quartz and biotite. Occasionally, its modal abundance reaches 5 vol.%. Tourmaline also occurs in cross-cutting veins. Minerals such as actinolite, chlorite, and calcite develop, as a rule, in fissures or replacing garnet and clinopyroxene.

Mineral inclusions in garnet and zircon

Since the clinozoisite-bearing rocks have been considerably altered by retrograde metamorphism, the main attention was given to mineral inclusions in garnets and zircons. As shown earlier (Shatsky & Sobolev, 1993; Sobolev *et al.*, 1991, 1994; Katayama *et al.*, 2000; Hermann *et al.*, 2001), the UHPM mineral inclusions are mostly preserved, solely in these minerals.

Zircon is present as an accessory mineral in all samples and occurs as rounded, slightly elongated grains measuring 100-150 μm, less frequently up to 250 μm, colourless or light-cream in colour. Concentric zonation and spottiness of the zircons are revealed by cathode luminescence. The following mineral inclusions are seen in zircon: biotite, phengite, kyanite, coesite, diamond, clinopyroxene, amphibole, quartz, carbonates and chlorite. It is noteworthy that zircon cores often contain clusters of non-identified mineral inclusions (Fig. 5 a, f). They do not exceed 2-3 μm in size, whereas large (up to 20-30 μm) inclusions are predominant at the rims (Fig. 5a). At the same time, there is no regularity in the spatial distribution of high- and low-pressure minerals in zircon. Intergrowths of mineral inclusions are quite rare. Such intergrowths are observed only in five zircon crystals out of about 2000 examined grains and they are garnet-clinopyroxene, garnet-biotite, clinopyroxene-amphibole, garnet-quartz and clinopyroxene-quartz (Table 3). In many cases, several mineral inclusions are detected within one grain of zircon: diamond and garnet, coesite and garnet, quartz and garnet, garnet and garnet. The occurrence of inclusions in the same zone suggests that they might have been trapped simultaneously. Occasionally, zircon itself forms inclusions in garnet, but in this case its grains are less than 30 μm in size, and we failed to observe inclusions in such zircons.

The garnet inclusions identified in zircons are small rounded grains measuring 10-20 and rarely up to 80 μm. As a rule, they are pale pink-coloured which distinguishes them from other mineral inclusions in the thin section. Garnet occurs in the cores of zircon crystals, as well as in the rims.

Clinopyroxene inclusions are detected in both garnet and zircon. Generally speaking, these are elongated crystals, and their size rarely exceeds 10 μm. Mica inclusions in zircon and garnet are represented by biotite and phengite. These inclusions typically measure up to 10 μm; therefore, most of them are colourless, and only large crystals of biotite are coloured brown. Sometimes they are

Table 4. Representative analyses of rock-forming mineraals and mineral inclusions from clinozoisite gneisses.

Sample	B93-6											
Mineral		Grt			Grt		Grt*	Bt	Cpx		Czo	Kfs
	18R1	18C	18R2	37R1	37C	37R2			C	R		
SiO_2	39.9	40.3	40.4	40.3	40.4	39.8	39.2	38.2	53.9	53.8	39.7	64.7
TiO_2	0.00	0.00	0.00	0.00	0.00	0.00	0.00	3.44	0.14	0.17	0.03	0.01
Al_2O_3	22.9	22.8	27.7	22.9	22.8	22.8	21.9	16.5	2.68	3.15	32.3	18.1
FeO	15.9	11.7	13.2	13.3	14.8	16.1	16.6	7.4	3.79	3.45	0.74	0.07
MnO	1.97	0.68	0.89	0.98	1.29	2.56	2.91	0.12	0.26	0.21	0.04	0.00
MgO	8.90	8.83	7.11	9.92	11.27	9.06	8.61	18.50	15.00	15.20	0.10	0.01
CaO	10.5	15.7	11.5	12.5	9.49	9.78	9.96	0.02	23.4	23.1	24.3	0.13
Na_2O	0.00	0.00	0.00	0.00	0.00	0.00	0.00	0.09	0.62	0.65	0.00	0.89
K_2O	0.00	0.00	0.00	0.00	0.00	0.00	0.00	9.94	0.00	0.01	0.01	15.5
Σ	100.06	100.01	100.74	100.01	100.00	100.04	99.29	94.19	99.78	99.77	97.18	99.30
Si	3.00	3.00	2.95	3.00	3.00	3.00	2.99	2.78	1.97	1.97	3.04	3.00
Ti	0.00	0.00	0.00	0.00	0.00	0.00	0.00	0.19	0.00	0.00	0.00	0.00
Al	2.03	2.00	2.38	2.01	2.00	2.02	1.98	1.41	0.12	0.14	2.92	0.99
Fe	1.00	0.73	0.80	0.83	0.92	1.01	1.06	0.45	0.12	0.11	0.05	0.00
Mn	0.13	0.04	0.06	0.06	0.08	0.16	0.19	0.01	0.01	0.01	0.00	0.00
Mg	1.00	0.98	0.77	1.10	1.25	1.02	0.98	2.01	0.82	0.83	0.01	0.00
Ca	0.85	1.25	0.90	1.00	0.76	0.79	0.82	0.00	0.92	0.91	1.99	0.01
Na	0.00	0.00	0.00	0.00	0.00	0.00	0.01	0.01	0.04	0.05	0.00	0.08
K	0.00	0.00	0.00	0.00	0.00	0.00	0.00	0.92	0.00	0.00	0.00	0.92
Fe/(Fe+Mg)	0.50	0.43	0.51	0.43	0.42	0.50	0.52	0.18	0.12	0.11		

*- Fine euhedral garnet

	Inclusions in garnet			Inclusions in zircon														
	B94-347	B95-42	B93-6	B94-156	B93-6					B94-369		B94-331(a)						
№	1	2	3	15-77	70-208	87-150	47-186	16-128	20-88	21-81	29-83	46-17	43-21	49-17*	49-18*	60-21**	41-8**	
Mineral	Chl	Amf	Pl	Cpx	Cpx	Cpx	Phe	Kfs	Chl	Bt	Bt	Phe	Bt	Grt	Grt	Grt	Grt	
SiO_2	31.2	48.1	59.2	52.4	53.3	55.3	53.4	65.3	31.7	37.8	38.7	51.1	38.9	40.6	39.3	39.9	41.1	
TiO_2	0.00	0.29	0.00	0.07	0.26	0.22	0.02	0.01	0.01	1.93	2.29	2.10	1.33	0.08	0.06	0.08	0.09	
Al_2O_3	14.6	14.3	25.6	8.3	12.9	16.4	25.5	18.3	16.9	15.2	17.5	24.7	16.4	22.3	21.6	21.7	22.2	
FeO	12.7	6.1	0.19	2.30	3.06	2.45	1.56	0.00	13.6	9.24	6.01	1.24	10.4	9.86	15.2	15.1	9.88	
MnO	0.15	0.08	0.01	0.13	0.27	0.26	0.07	0.00	0.29	0.25	0.17	0.01	0.27	0.44	1.84	1.64	0.42	
MgO	28.1	15.3	0.01	12.90	9.74	7.36	4.23	0.01	23.4	18.8	18.1	5.36	18.0	10.6	8.36	9.03	10.0	
CaO	0.17	11.87	7.56	21.5	16.84	12.4	0.19	0.12	0.05	0.02	0.07	0.00	0.00	15.7	12.7	12.0	15.9	
Na_2O	0.08	0.68	7.08	1.55	3.32	5.50	0.18	1.01	0.10	0.07	0.10	0.03	0.13	0.02	0.01	0.01	0.02	
K_2O	0.06	0.18	0.24	0.01	0.02	0.00	7.66	15.31	0.05	9.51	10.06	10.00	9.20	0.00	0.00	0.00	0.00	
Total	87.10	96.80	99.89	99.08	99.65	99.96	92.80	100.14	86.08	92.79	93.08	94.54	94.52	99.58	99.08	99.42	99.56	
Si	3.10	6.79	2.65	1.90	1.90	1.93	3.56	3.00	3.17	2.82	2.83	3.42	2.85	3.01	3.00	3.02	3.04	
Ti	0.00	0.03	0.00	0.00	0.01	0.01	0.00	0.00	0.00	0.11	0.13	0.11	0.07	0.00	0.00	0.00	0.01	
Al	1.71	2.39	1.35	0.36	0.54	0.68	2.00	0.99	1.99	1.33	1.51	1.95	1.41	1.95	1.94	1.94	1.94	
Fe	1.05	0.72	0.01	0.07	0.09	0.07	0.09	0.00	1.14	0.58	0.37	0.07	0.63	0.61	0.97	0.96	0.61	
Mn	0.01	0.01	0.00	0.00	0.01	0.01	0.00	0.00	0.02	0.02	0.01	0.00	0.02	0.03	0.12	0.11	0.03	
Mg	4.15	3.21	0.00	0.70	0.52	0.38	0.42	0.00	3.48	2.09	1.97	0.53	1.96	1.16	0.95	1.02	1.11	
Ca	0.02	1.80	0.36	0.84	0.64	0.46	0.01	0.01	0.01	0.00	0.01	0.00	0.00	1.25	1.04	0.97	1.26	
Na	0.02	0.19	0.61	0.11	0.23	0.37	0.02	0.09	0.02	0.01	0.01	0.00	0.02	0.00	0.00	0.00	0.00	
K	0.01	0.03	0.01	0.00	0.00	0.00	0.65	0.90	0.01	0.91	0.94	0.85	0.86	0.00	0.00	0.00	0.00	
Fe/(Fe+Mg)	0.20	0.18	0.88	0.09	0.15	0.16	0.17	0.11	0.25	0.22	0.16	0.11	0.24	0.34	0.50	0.48	0.36	

*- Garnets from the same zircon grain; 49-18 is located closer to the central part of the grain

**- Garnets occurring as inclusions in the same sample

intergrown with diamond, but these intergrowths are very tiny, 1-3 μm in size, and, thus, cannot be analysed by electron microprobe. The only plagioclase inclusion (An 35-40) was found in sample B93-6, occurring as an isometric grain 50 μm in size in the core of a garnet crystal. The other samples do not contain plagioclase, neither in matrix or as inclusions.

In the rocks of the Kokchetav Massif, coesite inclusions were found for the first time not only in zircons but also in garnets of the diamondiferous clinozoisite gneiss (Fig. 5g and 5i). Along with the coesite peak (521 cm^{-1}) in the Raman spectrum, there is a weak maximum corresponding to quartz. This is indicative of the initial stage of coesite-to-quartz transformation during retrogression. However, the number of grains between amounts of quartz and coesite in zircon differs from that in garnet even for the same sample. Thus, among the 570 examined garnet grains (B94-83), only 13 contain coesite and 52 contain quartz, whereas only

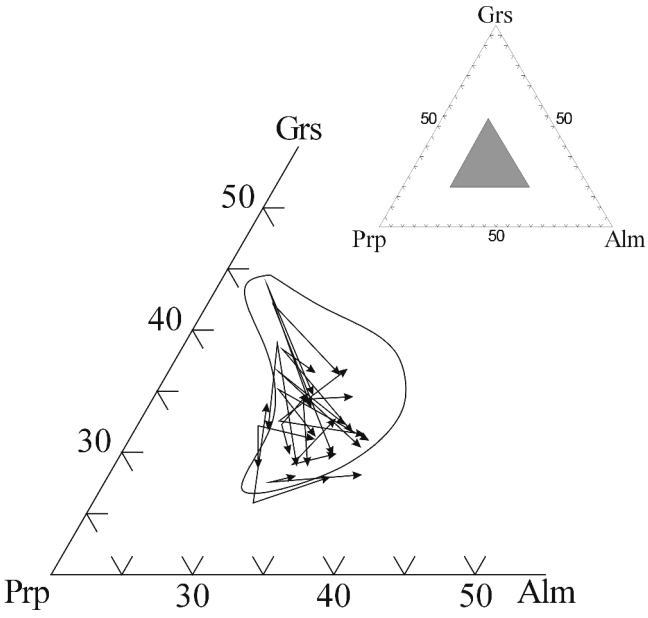

Fig. 6. Compositions of rock-forming garnets from clinozoisite gneiss (B93-6).

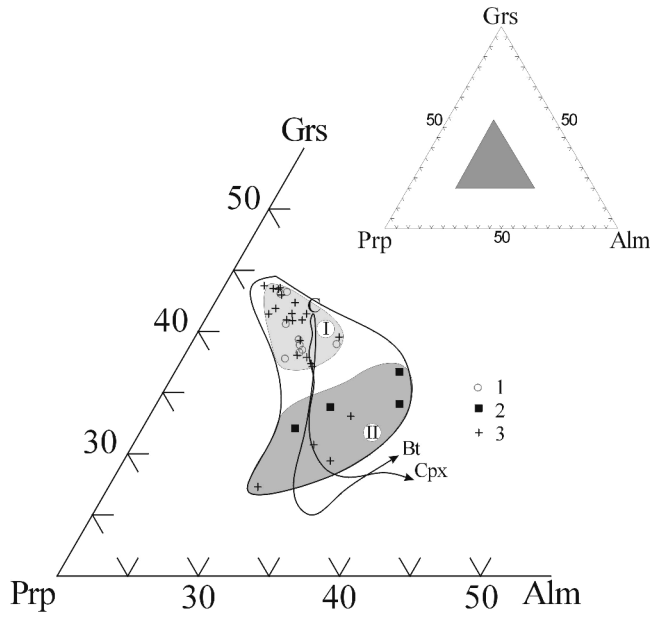

Fig. 7. Compositions of garnet inclusions (B93-6) from various assemblages: (1) high-pressure (Coe, Dia); (2) low-pressure (Qtz, Gr); (3) not informative. Lines showing the concentration profile in rock-forming garnet given in Fig. 10. I and II, corresponding to fields of compositions of high- and low-pressure garnets, respectively.

7 coesite inclusions and 2 quartz inclusions were identified after examining about 100 grains of zircon.

Carbon occurs in the gneisses as two polymorphous forms, namely graphite and diamond, which often coexist in the same sample. It should be noted that diamond is not found in graphite-free rocks. Nevertheless, the presence of graphite does not imply the presence of diamond. Two generations of graphite can be distinguished in the gneisses. Hexagonal graphite flakes (up to 20 μm), related to the first generation and associated with diamond, form inclusions in different minerals. In some cases, graphite surrounds diamond partly or completely, but their relationships cannot be convincingly established because of the minute size of the intergrowths of these minerals. The second-generation graphite occurs mainly in the intergranular space as large crystals up to 2-3 mm.

During an earlier study of the Kumdy-Kol deposit (Shatsky & Sobolev, 1993), diamond was found in garnet, zircon, clinopyroxene, micas, kyanite and chlorite. In the Barchi-Kol clinozoisite gneisses, it was identified in garnet, zircon, kyanite and quartz-clinozoisite symplectite, as well as in pseudomorphs of mica-carbonate aggregate after garnet. In previous studies, it has been shown (Shatsky *et al.*, 1998a) that a relationship exists between diamond morphology and petrographic rock type. Thus, diamonds in the garnet-pyroxene rocks are represented by reshaped cuboids: Reshaped cuboids and skeleton crystals of diamonds dominate in the carbonate rocks, whereas the predominant diamond morphology is cuboctahedral in the garnet-biotite gneisses. A complete morphological series (from reshaped cuboids to plane-faced octahedra) has been established in the clinozoisite gneisses from the Barchi-Kol area. The plane-faced octahedra are the main morphological type for gneisses containing clinozoisite as by single crystals (Fig. 5g and 5h). Gneisses with quartz-clinozoisite symplectite are dominated by reshaped cuboids. The distribution of graphite and diamond in samples is irregular. Garnets including only diamond, only graphite, or graphite and diamond, as well as grains containing none of the carbon polymorphs, may occur within the same thin section. Diamond morphology does not depend on the host mineral within one sample, *i.e.* it remains the same in garnet as well as in zircon, in kyanite, and in the quartz-clinozoisite symplectite.

Mineral chemistry

Analytical results given in Table 4 and Fig. 6 and 7 show that the rock-forming garnets and garnet inclusions are characterized by wide variations in composition: $Alm_{14-48}Sps_{0.3-11}Prp_{23-51}Grs_{15-47}$.

Garnet grains with maximal variations of composition from core to rim were profiled, and the results obtained show that their composition varies only in a narrow marginal zone (Fig. 8). The composition of small euhedral crystals of garnet corresponds to the composition of the marginal zones of larger grains. Numerous analyses of garnets from one thin section show that the garnets encountered over a small area (1 mm^2) display opposite types of zonation (Fig. 6), *i.e.*, the grossular component increases from core to rim in some grains and the opposite pattern is observed in others.

Aggregation gives rise to large garnet porphyroblasts often composed of several minute crystals. Various zones were analysed in one of these garnets (Fig. 8). It appeared

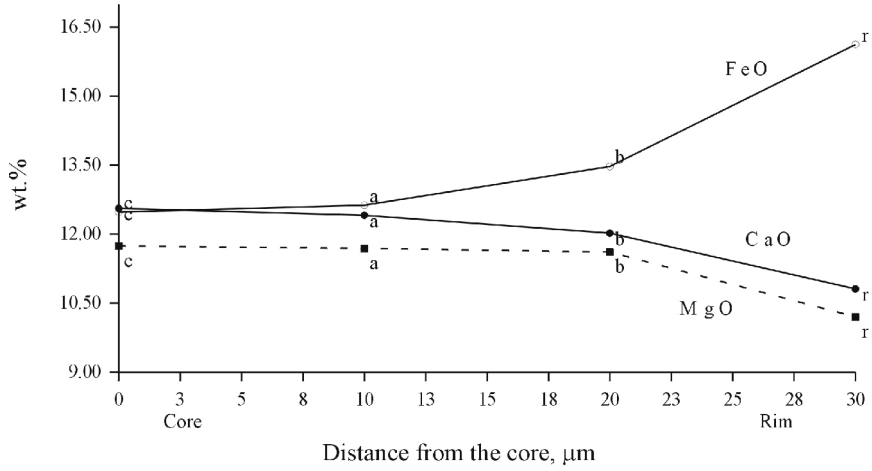

Fig. 8. Major element concentration profile of rock-forming garnet from clinozoisite gneiss (B94-347).

that the concentrations of Fe, Mn, Mg, and Ca in the core (marked C on Fig. 8) of a large porphyroblast correspond to compositions at its rim (marked R1 and R2 on Fig. 8). At the same time, the chemical compositions of the cores (centres marked C1 and C2 on Fig. 8) of individuals making up the porphyroblast are practically identical. A closer study of the zonation in garnets shows that some of them exhibit an intricate pattern of zonation, especially of MgO, whose origin is difficult to explain unambiguously (Fig. 9).

Since nearly all the samples contain garnets with inclusions of graphite and/or diamond , or with coexisting polymorphs, we compared the compositions of garnets with (N_1 = 15) or without diamond inclusions (N_2 = 17). No significant differences were found by statistical treatment.

In zircons, garnet is one of the most abundant mineral inclusions. Occasionally, it coexists with diamond, coesite, quartz and chlorite. The grossular content in garnets from high-pressure assemblages (with diamond and coesite) is higher than in low-pressure assemblages (with quartz and graphite) (Fig. 7). It is to be noted that independent estimates of pressures are impossible for most garnet inclusions because of the absence of indicator minerals. 8 garnets of 36, *i.e.* 22 %, fall within the low-pressure composition field (Fig. 7). This suggests that about 80 % of garnets nucleated during the peak of metamorphism.

The compositions of clinopyroxenes from the matrix and occurring as inclusions in garnet are essentially different from clinopyroxenes included in zircon (Table 4). The clinopyroxene inclusions in zircons contain more

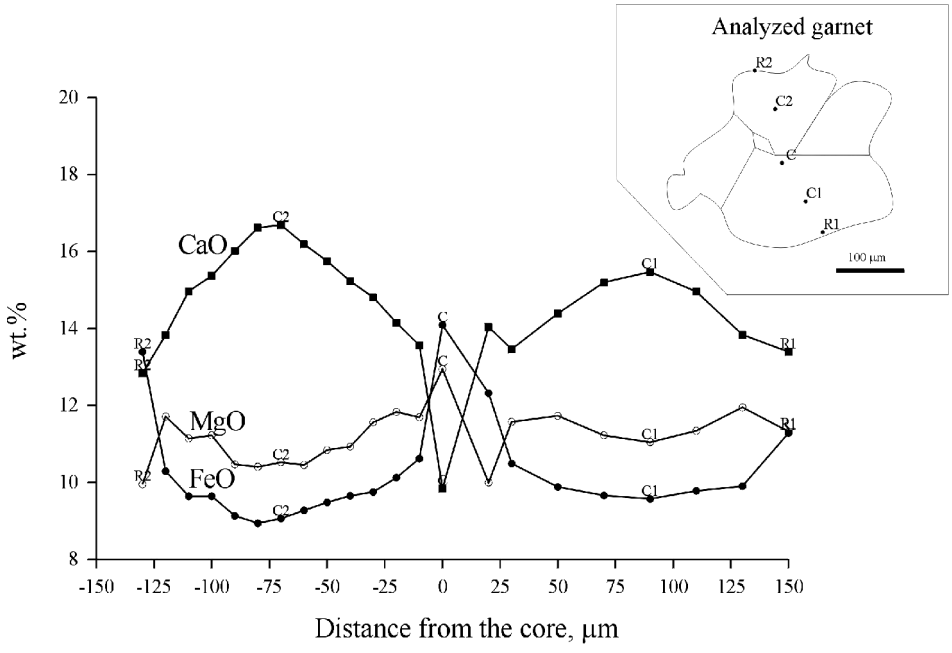

Fig. 9. Major-element concentration profile of a large garnet crystal consisting of several minute individual grains.

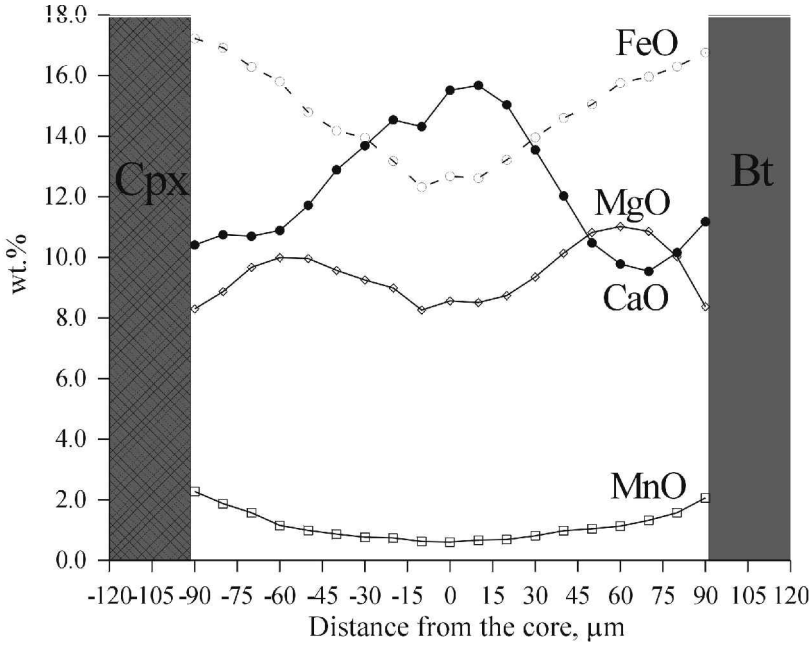

Fig. 6. Compositions of rock-forming garnets from clinozoisite gneiss (B93-6).Fig. 10. Distribution of FeO, MnO, MgO, and CaO in a crystal of garnet in contact with clinopyroxene (left) and biotite (right) (B93-6).

jadeite (X_{Jd} < 37 mol.%) compared with the rock-forming clinopyroxenes (X_{Jd} < 4.6 mol.%) or the clinopyroxene inclusions analysed in garnets (X_{Jd} < 10 mol.%). An intergrowth of clinopyroxene with amphibole was analysed in one of the inclusions. An admixture of potassium (0.1 % K_2O) was found in clinopyroxene inclusions in zircons. In another inclusion, we detedted an intergrowth of clinopyroxene and quartz. This same inclusion is characterized by the maximum content of jadeite end-member – 37 mol.%.

The biotites detected as inclusions in zircons and garnets are richer in iron than the rock-forming biotites. Thus, in sample B94-369, the rock-forming biotites have a Fe/(Fe+Mg) ratio of 22-26 %, whereas biotite inclusions yield a ratio of 25-33 %. Phengites with Si varying from 3.41 to 3.56 p.f.u. were analysed in samples B93-6 and B95-42 in zircon (Table 4).

Table 4 lists the compositions of the chlorites found as inclusions in zircon. Like all the above-mentioned minerals, chlorite is characterised by moderate variations in composition (see Table 4).

Although low-pressure minerals such as chlorite and quartz are found as inclusions in zircons, none of them exhibit intergrowths with diamond.

The analysed inclusions of carbonate in zircons and garnets are magnesian calcite containing up to 12 mol.% $MgCO_3$ (Fig. 5d). Veinlets of calcite are observed in the matrix of clinozoisite rocks. In this case the content of $MgCO_3$ does not exceed 3 mol.%.

Estimation of metamorphic conditions

Modern methods for estimating the physicochemical conditions of formation of metamorphic rocks use the software packages TWQ1.02, WEBINVEQ and THERMOCALC, which include the consistent thermodynamic databases of various authors (Berman, 1988; Holland & Powell, 1998). To use these programs, it is necessary to define the compositions of the phases coexisting under equilibrium. Usually, it is very difficult to do this for UHPM mineral assemblages having a complicated metamorphic history. A formal application of these methods will yield P-T values, but, as a rule, there do not correspond to any particular stage: Therefore, the estimates are difficult to interpret in a meaningful way. The conditions of formation of the assemblages Grt-Cpx-Czo-Ky-Bt-Kfs-Qtz, Grt-Cpx-Czo-Bt-Kfs-Qtz, and Grt-Czo-Bt-Kfs-Qtz observed in clinozoisite gneisses were determined by means of the THERMOCALC package (compositions of coexisting minerals are given in Table 4). The calculated temperatures and pressures for the first and second assemblages are 950°C at 20 kbar and 800°C at 6.5 kbar, respectively. Moreover, the third and most typical assemblage of the majority of samples, provided no information for the reconstruction of P and T. Since only one independent reaction (Alm+Phl = Prp+Ann) exists for the Grt-Czo-Bt-Kfs-Qtz assemblage, it is impossible to determine simultaneously both temperature and pressure.

Thus, to estimate parameters of the high-pressure stage of metamorphism, we used relict assemblages preserved as inclusions in garnets and zircons. The high-pressure minerals reliably recognised in the clinozoisite gneisses are garnet, phengite, biotite and clinopyroxene.

Evidence for the high-pressure conditions of biotite formation is given by its intergrowth with the diamond observed as inclusions in zircon and garnet. Garnet contains diamond, and occasionally its intergrowths with diamond or coesite are found as inclusions in zircons.

Table 5. Compositions of pyroxenes and biotites occuring as inclusions within garnet grains and calculated temperature estimates (at P = 10 kbar) and K_D value.

	Grt-Cpx								Grt-Bt											
Thermometer	B94-347						B94-156		B94-347						B94-156				B95-42	
Mineral	Grt1	Cpx1	Grt2	Cpx2	Grt3	Cpx3	Grt1	Cpx1	Grt1	Bt1	Grt2	Bt2	Grt3	Bt3	Grt1	Bt1	Grt2	Bt2	Grt1	Bt1
SiO_2	39.9	52.56	40.7	52.43	40.6	53.35	41.0	52.76	40.2	37.32	40.6	37.98	40.8	37.37	40.3	39.84	40.1	37.80	40.3	38.35
TiO_2	0.05	0.14	0.07	0.13	0.10	0.12	0.12	0.18	0.06	1.91	0.04	1.67	0.05	1.55	0.08	2.64	0.11	1.13	0.05	2.28
Al_2O_3	22.4	5.33	22.3	4.90	22.2	5.80	22.6	5.84	22.1	16.77	22.4	17.02	22.7	16.53	22.2	17.35	21.9	17.42	22.4	17.19
FeO	16.4	2.46	12.1	3.78	12.0	2.31	8.5	1.77	15.6	9.06	11.6	9.40	10.0	9.96	11.9	6.48	12.7	9.52	12.5	9.38
MnO	0.81	0.04	0.32	0.10	0.26	0.03	0.45	0.03	0.63	0.11	0.308	0.11	0.292	0.10	1.12	0.14	1.12	0.08	0.59	0.20
MgO	8.94	15.01	12.1	14.48	11.9	14.63	10.1	15.05	10.4	18.03	10.9	18.67	10.8	19.26	9.7	18.50	9.42	18.37	9.42	16.69
CaO	11.6	22.11	12.3	22.58	13.4	21.41	17.2	23.48	10.9	0.02	14.0	0.06	15.5	0.04	14.1	0.11	14.2	0.11	14.7	0.03
Na_2O	0.00	1.55	0.00	0.86	0.04	1.73	0.02	0.62	0.00	0.10	0.00	0.11	0.00	0.09	0.01	0.18	0.04	0.16	0.00	0.12
K_2O	0.00	0.05	0.00	0.01	0.00	0.13	0.00	0.01	0.00	9.26	0.00	8.96	0.00	8.88	0.05	9.06	0.07	9.27	0.00	9.00
Total	99.98	99.25	99.88	99.26	100.57	99.51	99.94	99.75	99.91	92.58	99.92	93.98	99.93	93.78	99.51	94.30	99.63	93.86	99.93	93.24
Si	3.00	1.92	3.01	1.92	2.99	1.93	3.02	1.91	3.01	2.84	3.01	2.84	3.00	2.81	3.01	2.91	3.01	2.84	3.00	2.83
Ti	0.00	0.00	0.00	0.00	0.01	0.00	0.01	0.00	0.00	0.11	0.00	0.09	0.00	0.09	0	0.15	0.01	0.06	0.00	0.13
Al	1.99	0.23	1.94	0.21	1.92	0.25	1.96	0.25	1.95	1.50	1.95	1.50	1.97	1.46	1.96	1.49	1.94	1.54	1.97	1.49
Fe	1.03	0.08	0.75	0.12	0.74	0.07	0.52	0.05	0.98	0.58	0.72	0.59	0.61	0.63	0.75	0.40	0.8	0.60	0.78	0.58
Mn	0.05	0.00	0.02	0.00	0.02	0.00	0.03	0.00	0.04	0.01	0.02	0.01	0.02	0.01	0.07	0.01	0.07	0.01	0.04	0.01
Mg	1.00	0.82	1.33	0.79	1.31	0.79	1.11	0.81	1.16	2.04	1.21	2.08	1.19	2.16	1.08	2.01	1.05	2.05	1.05	1.83
Ca	0.93	0.86	0.97	0.89	1.06	0.83	1.35	0.91	0.88	0.00	1.11	0.01	1.22	0.00	1.13	0.01	1.14	0.01	1.17	0.00
Na	0.00	0.11	0.00	0.06	0.01	0.12	0.00	0.04	0.00	0.01	0.00	0.02	0.00	0.01	0	0.03	0.01	0.02	0.00	0.02
K	0.00	0.00	0.00	0.00	0.00	0.01	0.00	0.00	0.00	0.90	0.00	0.85	0.00	0.85	0	0.84	0.01	0.89	0.00	0.85
K_D	**11.19**		**3.83**		**6.39**		**7.16**		**2.98**		**2.12**		**1.79**		**3.53**		**2.62**		**2.37**	
T^0C (Powell,1985)	657		988		828		888													
T^0C (Hoges & Spear, 1981)									775		940		1043		669		808		859	
T^0C (Ellis & Green,1979)	676		996		842		898													
T^0C (Ai,1994)	452		793		617		665													

Detection of Si-rich phengite (up to 3.56 p.f.u. Si) may be indicative of higher pressures (Massonne & Schreyer, 1987), but it is not possible to estimate the precise P-T conditions of its formation.

To estimate metamorphic temperatures, we used garnet-clinopyroxene (Ellis & Green, 1979; Powell, 1985) and garnet-biotite (Hodges & Spear, 1981) geothermometers. We analysed the parts of grains that were in contact since only these could likely be in equilibrium. In the following, unless otherwise specified, the pressure was taken as equal to 10 kbar, which corresponds to the uplift of rocks to mid-crust level. According to the garnet-clinopyroxene geothermometer, the temperature range for samples B93-6 and B95-42 is 750-900°C and 950-1120°C, respectively, and according to the garnet-biotite thermometer, it is 630-1190°C. The temperatures obtained by these two thermometers are rather different. A possible reason is the high grossular content in the garnets.

The P-T conditions of the high-pressure stage of metamorphism were determined by the technique described in Shatsky *et al.* (1995). Since this approach was used earlier for examining the diamondiferous rocks from the Kumdy-Kol deposit, we used it here for correct comparison. To estimate temperatures, we analysed clinopyroxene and mica inclusions in garnet. The data obtained are given in Table 5. It is remarkable that the size of most inclusions does not exceed 20 μm, *i.e.* we cannot conclude that the analysed compositions correspond to the moment of trapping. Most likely, the exchange reactions proceeded also during retrogression down to 500°C, when the coefficients of diffusion become very small (about 10^{-19} cm^2/s). But even in this case, the scatter in distribution coefficients (K_D) appears to be too wide (Table 5). A clinopyroxene-quartz intergrowth, yielding a temperature of formation of 990°C, was identified in the core of one of the garnet crystals (B94-347). In another garnet grain of the same sample, a clinopyroxene inclusion occurs in the rim, and the temperature of its formation corresponds to 680°C. In Table 3, we report analyses of the intergrowths of clinopyroxene with garnet (Fig. 5e, B94-369)as well as biotite with garnet (B94-369) occurring as inclusions in zircon. The temperatures for the garnet-clinopyroxene and garnet-biotite pairs are 880° and 720°C, respectively. Thus, the most reliable estimates of temperatures for the different stages of metamorphism may be obtained from mineral pairs that are spatially very close but isolated by an unreactive medium. The most appropriate material for this purpose are inclusions of garnet, clinopyroxene and biotite in zircon coexisting within the same growth zone.

The mineral assemblages present in the rocks, Qtz-Chl-Mu and Cal-Act-Chl, suggest that the latest retrograde stage corresponds to greenschist facies conditions.

Discussion

Two garnet inclusions ($Alm_{38.17}Prp_{20.91}Grs_{40.92}$ and $Alm_{30.87}Prp_{35.30}Grs_{33.83}$) from one grain of zircon cover nearly the whole range of the garnet compositions analysed in the zircons of this sample (Table 4). Although the distance between them is 50 μm, they occur in different zones of the zircon grain, as revealed by cathode luminescence (Fig. 5c). It noteworth that the garnet inclusion near the core contains more calcium, *i.e.* as zircon grew, the

garnet composition became increasingly poorer in Ca component. A similar pattern of distribution is also observed for Ca in the rock-forming garnets. The high grossular contents of garnet inclusions from coesite- and diamond-bearing assemblages, as well as the low grossular contents in garnet associated with quartz and graphite, suggest that the growth of zircons and rock-forming garnets continued during the decompression stage.

Since garnet is often in contact with different minerals (biotite, clinopyroxene, clinozoisite, quartz and K-feldspar), the rim compositions may differ considerably even within one grain. The similarity in composition between small garnets and the rims of larger garnets implies that the small garnets nucleated and grew during retrogression. Zonation is preserved even in the smallest crystals (< 30 μm), indicating a high rapid of temperature decrease. The duration of mineral-forming processes under ultrahigh pressure conditions were estimated from the diffusion model (Lepezin & Korolyuk, 1984):

$$C(x,t) = \overline{C} + \frac{1}{x}\sum_{n=1}^{\infty} B_n \sin(\lambda_n x)\exp[-\lambda_n^2 \int_0^t D(z)dz] \quad (1).$$

where $\overline{C} = \frac{3}{r_k^3}\int_0^{r_k} N(x,0)x^2 dx$,

$$Bn = \frac{4\lambda_n}{2\lambda_n r_k - \sin(2\lambda_n r_k)} \int_0^{rk} N(x,0)x\sin(\lambda_n x)dx,$$

$tg(\lambda_n r_k) - \lambda_n r_k = 0$, N(x,0) is the initial distribution, r_k is the crystal radius, D is the coefficient of diffusion, and t is time.

The temperature dependence of the diffusion coefficient of Ca in Fe-Mg garnets is taken from experimental data (Freer & Edwards, 1999)

$$\tilde{D} = 1.22^{+6.44}_{-1.00} * 10^{-6} \exp(\frac{-270.4 \pm 19.3kJ}{RT}) \text{ (m}^2\text{/c)}.$$

Since we do not know whether the zonation in garnet from the clinozoisite gneisses is caused by growth or by diffusion, or even growth and diffusion simultaneously, the diffusion problem can be formulated as follows: What would be the cooling rate (down to T_c = 500°C) of these rocks necessary to maintain the concentration profile presently recorded in garnet? The observed distributions, N(x,0), of FeO, MnO, MgO and CaO in garnet crystals were approximated by orthogonal polynomials and used in equation (1). The estimated duration of the thermal effect in this model depends on initial temperature. Thus, at T_0 = 1000°C the duration is less than 100 years, at T_0 = 800°C it is 10,000 years, and at T_0 = 700°C it is 100,000 years. In our case, we used the lowest diffusion coefficients. Therefore, the duration of crystallisation and subsequent annealing processes must be less than 100,000 years.

One of the distinctive features of the rocks in question is the presence of quartz-clinozoisite symplectites. According to experimental studies (Boettcher, 1970; Schmidt & Poli, 1994), the stability field of clinozoisite is limited by the reaction Zo+Qzt = Grs+L, with the curve having a positive slope, *i.e.* as the pressure increases, the stability field of clinozoisite with quartz expands up to the quartz-coesite phase transition. This reaction has not been studied experimentally at higher pressures. According to our temperature estimates for the high-pressure stage (900-950°C), the quartz-clinozoisite assemblage should be replaced by garnet in equilibrium with the melt. According to experimental data (Boettcher, 1970), melting should also be observed in the clinozoisite-kyanite-quartz assemblage at pressures exceeding 14 kbar and temperatures of 800°C. The presence of melt in the clinozoisite gneisses could account for the crystallisation of zircon and garnet with decreasing pressure and temperature, but direct evidence of melting (melt inclusions) has been found in any of the minerals.

The high jadeite content in clinopyroxene inclusions in the quartz-bearing assemblage suggests Cpx formation by plagioclase decomposition during a prograde stage. The low concentrations of Na in the rocks indicate an insignificant amount of plagioclase in the protoliths, which in turn accounts for the scarcity of Na-rich clinopyroxenes. Since the rock-forming clinopyroxenes (Na-poor) differ drastically in composition from the clinopyroxene (Na-rich) inclusions, the time of formation of the Na-poor clinopyroxenes remains an open question. Most likely, their growth took place after the complete disappearance of plagioclase from the system.

Nadezhdina & Posukhova (1990) used the scarcity of plane-faced diamond octahedra as evidence for the metastable growth of diamond. However, their hypothesis was rejected when samples of clinozoisite gneisses were found in which the dominant form of diamond was octahedral. The whole-rock compositions of clinozoisite gneisses (Table 1) cover a wide range from metapelites to silicate-carbonate rocks. Thus, neither bulk composition nor the modal composition of the studied rocks has any effect on the morphology of the diamond. As mentioned above, the samples containing single crystals of clinozoisite are dominated by plane-faced diamond crystals, whereas the rocks containing clinozoisite-quartz symplectite are dominated by reshaped cuboids. An explanation may be provided from the following model. In the first case, diamond crystallisation occurs in a closed system, *i.e.* as the reaction proceeds, carbon-supersaturation decreases and plane-faced crystals form. In the second case, the system is open, and the degree of carbon-supersaturation is determined by the relations between the matter supplied and consumed during the diamond growth. At the same time, it would be reasonable to assume that the diamond morphology is affected mainly by the amount of a fluid or a melt. The presence of fluid determines the degree of completeness of the reaction leading to the origin and growth of diamonds in metamorphic rocks. Support for this hypothesis comes from the fact that segments with fibrous fabric exist even in octahedral crystals (Shatsky *et al.*, 1998). This allows us to link the formation of plane-face octahedra with the reshaping of cuboids.

Conclusions

The above study leads to the following conclusions:

1. The conditions of high-pressure metamorphism of clinozoisite gneisses is the Barchi-Kol area do not differ

from those in the Kumdy-Kol deposit, and correspond T = 950-1000°C (according to garnet-clinopyroxene geothermometers) at a pressure of > 40 kbar.
2. The crystallisation of some grains of zircon and garnet began at the peak of metamorphism (P > 40 kbar and T = 950-1000°C) and continued during the decrease in temperature and pressure down to 10-12 kbar and 650-750°C. This fact should be taken into account in interpretating the ages obtained by U-Pb and Sm-Nd methods.
3. The investigation revealed no dependence of diamond crystal morphology on P-T conditions of metamorphism or chemical composition of the rocks. This suggests that the main factor governing diamond morphology is the amount of fluid phase or melt, which accounts for the different degrees of completeness of cuboid reshaping.
4. The duration of retrograde metamorphism, as estimated from zonation in garnets of diamondiferous rocks, is no more than 100,000 years. The preservation of coesite both in grains of zircon and garnet moreover indicates a short period during which the rocks were at high temperatures in the stability field of quartz.

Acknowledgments: We are very grateful to L.L. Perchuk and V.V. Reverdatto for constructive reviews of an earlier version of the manuscript. Financial support was given by the Fund of the General Director of UIGGM SB RAS and the Russian Fund for Fundamental Research (N 01-05-65093 and 01-05-06252).

References

Ai, Y. (1994): A revision of the garnet-clinopyroxene Fe^{2+}-Mg exchange geothermometer. *Contrib. Mineral. Petrol.*, **115**, 4, 465-473.

Berman, R.G. (1988): Internally-consistent thermodynamic data for minerals in the system Na_2O-K_2O-CaO-MgO-FeO-Fe_2O_3-Al_2O_3-SiO_2-TiO_2-H_2O-CO_2. *J. Petrol.*, **29**, 445-522.

Boettcher, A.L. (1970): The system CaO-Al_2O_3-SiO_2-H_2O at High Pressure and Temperatures. *J. Petrol.*, **11**, 337-379.

Chopin, C. & Sobolev N.V. (1995): Principal mineralogical indicators of UHP in crustal rocks. *in* "Ultrahigh pressure metamorphism", Coleman R.G., Wang X., eds. Cambridge University Press, Cambridge, 96-131.

Claoue-Long, J.C., Sobolev, N.V., Shatsky, V.S., Sobolev, A.V., 1991. Zircon response to diamond-pressure metamorphism in the Kokchetav massif, USSR. *Geology*, **19**, 7, 710-713.

Cullers, R.L. (1994): The controls on the major and trace element variation of shales, siltstones, and sandstones of Pennsylvanian-Permian age from uplifted continental blocks to platform sediment in Kansas, USA. *Geochim. Cosmochim. Acta*, **58**, 4955-4972.

De Corte, K., Cartigny, P., Shatsky, V.S., Sobolev, N.V., Javoy, M. (1998): Evidence of inclusions in metamorphic microdiamonds from Kokchetav Massif, Northern Kazakhstan. *Geochim. Cosmochim. Acta*, **62**, 3765-3773.

Dobretsov, N.L., Sobolev, N.V., Shatsky, V.S., Coleman, R.G., Ernst, W.G. (1995): Geotectonic evolution of diamondiferous paragneisses Kokchetav complex, Northern Kazakhstan - the geologic enigma of ultrahigh- pressure crustal rocks within Phanerozoic foldbelt. *The Island Arc*, **4**, 267-279.

Dobretsov, N.L., Theunissen, K., Smirnova, L. (1998): Structural and geodynamic evolution of diamond-bearing metamorphic rocks of Kokchetav massif, Kazakhstan. *Geologiya i Geofizika*, **39**, 1645-1666 (in Russian). English Translation: Russian Geology and Geophysics, **39**, 1650-1661.

Ekimova, T.E., Lavrova, L.D., Nadezhdina, E.D., Petrova, M.A., Pechnikov, V.A. (1994): Conditions of the formation of the Kumdy-Kol' diamond deposit, Northern Kazakhstan. *Geologiya Rudnykh Mestorozhdenii (Geology of Ore Deposits)*, **36**, 455-465 (in Russian).

Ellis, D.J. & Green, D.H. (1979): An experimental study of the effect of Ca garnet- clinopyroxene, Fe-Mg exchange equilibria. *Contrib. Mineral. Petrol.*, **71**, 13-22.

Freer R. & Edwards A. (1999): An experimental study of Ca (Fe-Mg) interdiffusion in silicate garnets. *Contrib. Mineral. Petrol.*, **134**, 370-379.

Hermann, J., Rubatto, D., Korsakov, A., Shatsky, V.S. (2001): Multiple zircon growth during fast exhumation of diamondiferous, deeply subducted continental crust (Kokchetav Massif, Kazakhstan). *Contrib. Mineral. Petrol.*, **141**, 66-82.

Hodges, K.V. & Spear, F.S. (1981): Geothermometry, geobarometry, garnet close temperatures and the Al_2SiO_5 triple point. *Eos, Transactions, Am. Geophys. Union*, **62**, 1060.

Holland, T.J.B. & Powell, R. (1998): An internally-consistent thermodynamic data set for phases of petrological interest. *J. metamorphic Geol.*, **16**, 309-343.

Katayama, I., Zayachkovsky, A.A., Maruyama, S. (2000): Prograde pressure-temperature records from inclusions in zircons from rocks of the Kokchetav ultrahigh-pressure-high-pressure massif, northern Kazakhstan. *The Island Arc*, **9**, 417-427.

Korsakov, A.V., Shatsky, V.S., Sobolev, N.V. (1998): The first finding of coesite in eclogites of the Kokchetav massif. *Doklady Akademii Nauk*, **360**, 77-81.

Kretz, R. (1983): Symbols of rock-forming minerals. *Am. Mineral.*, **68**, 277-279.

Lavrova, L.D., Pechnikov, V.A., Petrova, M.A., Zayachkovsky, A.A. (1996): Geology of the Barchi-Kol diamond area. *Otechestvennaya Geologiya*, **12**, 20-27 (in Russian).

Lepezin G.G. & Korolyuk V.N. (1984): Growth dynamics of zonal garnets in divariant paragenesis. *Geologiya i Geofizika*, **25**, 116-126 (in Russian). English Translation: Soviet Geology and Geophysics, **25**, 111-121.

Massago, H. (2000): Metamorphic petrology of the Barchi-Kol metabasites, western Kokchetav ultrahigh-pressure-high-pressure massif, northern Kazakhstan. *The Island Arc*, **9**, 358-378.

Massonne, H.J. & Schreyer, W. (1987): Phengite geobarometry based on the limiting assemblage with k-feldspar, phlogopite and quartz. *Contrib. Mineral. Petrol.*, **96**, 212-224.

Nadezhdina, E.D. & Posukhova, T.V. (1990): Morphology of diamond crystals from metamorphic rocks. *Mineralogicheskii Zhurnal*, **12**, 3-15 (in Russian).

Powell, R., (1985): Regression diagnostic and robust regression in geothermometer/ geobarometer calibration: the garnet-clinopyroxene geothermometer revisited. *J. metamorphic Geol.*, **3**, 231-243.

Shatsky, V.S., Sobolev, N.V. (1993): Some aspects of the diamond formation in metamorphic rocks. *Doklady Akademii Nauk*, **331**, 217-219 (in Russian).

Shatsky, V.S., Sobolev, N.V., Zayachkovsky, A.A., Zorin, Yu.M., Vavilov, M.A. (1991): A new occurrence of microdiamonds in metamorphic rocks as a proof of the regional nature of ultra-

high pressure metamorphism in the Kokchetav Massif. *Doklady Akademii Nauk SSSR*, **321**, 189-193 (in Russian).

Shatsky, V.S., Sobolev, N.V., Vavilov, M.A. (1995): Diamond-bearing metamorphic rocks of the Kokchetav massif (Northern Kazakhstan). *in* "Ultrahigh pressure metamorphism", Coleman R.G., Wang X., eds. Cambridge University Press, Cambridge, 427-455.

Shatsky, V.S., Rylov, G.M., Efimova, E.S., De Corte, K., Sobolev, N.V. (1998a): Morphology and real structure of microdiamonds from metamorphic rocks of the Kokchetav Massif, kimberlites, and alluvial placers. *Geologiya i Geofizika*, **39**, 942-956 (in Russian). English Translation: Russian Geology and Geophysics, **39**, 949-961.

Shatsky, V.S., Theunissen, K., Dobretsov, N.L., Sobolev, N.V. (1998b): New indication of ultrahigh-pressure metamorphism in the mica schists of the Kulet site of Kokchetav massif (North Kazakhstan). *Geologya i geofizika*, **39**, 1039-1044 (in Russian). English Translation: Russian Geology and Geophysics, **39**, 1041-1046.

Shatsky, V.S., Jagoutz, E., Sobolev, N.V., Kozmenko, O.A., Parkhomenko, V.S., Troesch, M. (1999): Geochemistry and age of ultrahigh pressure metamorphic rocks from the Kokchetav massif (Northern Kazakhstan). *Contrib. Mineral. Petrol.*, **137**, 185-205.

Schmidt, M.W. & Poli, S. (1994): The stability of lawsonite and zoisite at high pressure as: Experiments in CASH to 92 kbar and implications for presence of hydrous phase in subducted lithosphere. *Earth Planet. Sci. Letters*, **124**, 105-118.

Sobolev, N.V. & Shatsky, V.S. (1987): Inclusions of carbon minerals in garnets of metamorphic rocks. *Geologiya i Geofizika*, **7**, 77-80 (in Russian). English Translation: Soviet Geology and Geophysics, **28**, 69-71.

– , – (1990): Diamond inclusions in garnets from metamorphic rocks: a new environment for diamond formation. *Nature*, **343**, 742-746.

Sobolev, N.V., Shatsky, V.S., Vavilov, M.A., Goryainov, S.V. (1991): Coesite inclusion in zircon of diamondiferous gneisses of the Kokchetav Massif: the first finding of coesite in metamorphic rocks on the territory of the USSR. *Doklady Akademii Nauk SSSR*, **321**, 184-188 (in Russian).

Sobolev, N.V., Shatsky, V.S., Vavilov, M.A., Goryainov, S.V. (1994): Zircon of high-pressure metamorphic rocks from folded regions as a unique container of inclusions of diamond, coesite, and coexisting minerals. *Doklady Akademii Nauk*, **334**, 488-492 (in Russian).

Theunissen, K., Dobretsov, N.L., Korsakov, A., Travin, A., Shatsky, V.S., Smirnova, L., Boven, A. (2000): Two contrasting petrotectonic domains in the Kokchetav Megamelange (north Kazakhstan): difference in exhumation mechanisms of ultrahigh-pressure crustal rocks, or a result of subsequent deformation? *The Island Arc*, **9**, 428-438.

Zhang, R.Y., Liou, J.G., Ernst, W.G., Coleman, R.G., Sobolev, N.V., Shatsky, V.S. (1997): Metamorphic evolution of diamond-bearing and associated rocks from Kokchetav massif, northern Kazakhstan. *J. metamorphic Geol.*, **15**, 479-496.

Received 16 May 2001
Modified version received 6 February 2002
Accepted 6 March 2002